

## Lateral Resolution Enhancement in Confocal Self-interference Microscopy with Commercial Calcite Plate

DongKyun Kang<sup>\*</sup>, HongKi Yoo, SeungWoo Lee, and Dae-Gab Gweon

*Nano Opto Mechatronics Lab., Dept. of Mechanical Engineering KAIST, Guseong-dong, Yuseong-gu, Daejeon, KOREA*

(Received January 27, 2005 : revised March 11, 2005)

In light microscopy, spatial resolution is limited by diffraction effect. Confocal microscopy has improved resolutions in both lateral and axial directions, but these are still limited by diffraction effect. Confocal self-interference microscopy (CSIM) uses interference between two perpendicularly polarized beams to enhance lateral resolution. In previous research, we proposed a calcite plate with its optic-axis perpendicular to the propagation angle and one of the boundary surfaces of the plate. This type of plate is not widely used to our knowledge. In this paper, we change the calcite plate to more common one, which is commercially available. This calcite plate has its optic axis in the plane of incidence. We analyze the characteristics of this calcite plate and numerically compare the performances of CSIM in previous research and CSIM with the commercial calcite plate. Numerical results show improved performance when using the commercial calcite plate

*OCIS codes* : 180.1790, 260.1440, 260.3160, 350.5730, 080.2740

### I. INTRODUCTION

Light microscopy has been an essential tool in many fields of science and engineering. Since confocal microscopy, which is also light microscopy, has optical sectioning ability and improved lateral resolution, it has been widely used in biological, medical and material-related researches [1]. However, as does other light microscopy, confocal microscopy has limited fields of application, due to its diffraction-limited resolution.

There have been several studies on improving resolution in confocal microscopy. Frequency-domain confinement was used to narrow the central lobe of the point-spread function (PSF) [2]. Pupil plane filters were designed to achieve superresolution in the lateral direction [3-5]. 4pi optics was used to improve both the axial and the lateral resolution [6]. Although these studies showed a great improvement of the lateral resolution, resulting imaging systems were often complicated and heights of sidelobes were sometimes increased.

In previous research, we proposed confocal self-interference microscopy (CSIM) [7]. CSIM uses birefringence material to separate two perpendicularly polarized beams and to make phase difference between these two beams. Since the phase difference changes as the incidence angle onto the calcite plate changes, CSIM can generate the interference pattern in the lateral coord-

inate of the specimen. In previous research, we proposed to use calcite plate with its optic axis perpendicular to the direction of propagation and one of the boundary surfaces of the plate (Type A calcite plate). To our knowledge, this type of calcite plate is not widely used. Instead, calcite plate with its optic axis in the plane of incidence and having non-zero angle with respect to the boundary surface (Type B calcite plate) is commonly used. This type of the calcite plate is widely used for beam displacing.

In this paper, we propose CSIM with Type B calcite plate. We analyze the characteristic of this type of calcite plate, and numerically compare the performances of CSIM with Type A and Type B calcite plates.

### II. PRINCIPLE OF CSIM

The schematic diagram of CSIM is shown in Fig. 1. A light beam from a He-Cd laser enters spatial filtering and beam expanding optics, which is composed of an objective lens-quality lens, a pinhole and an achromat lens. The light beam has wavelength of 442nm and is vertically polarized. The wavelength of the laser is chosen relatively short to further enhance the lateral resolution. It is chosen longer than near-violet wavelength to achieve fair qualities of optical components,

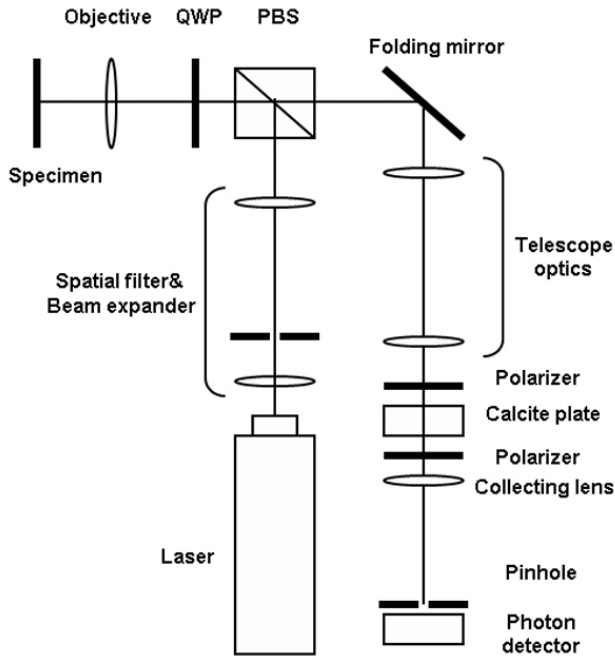


FIG. 1. Schematic diagram of CSIM.

since optical performance in near violet wavelength is poorer than that in longer wavelength.

Since the light beam is vertically polarized, the beam is reflected to the left by the polarized beam splitter (PBS). The beam is focused onto the specimen by the objective lens and the reflected beam from specimen is collected by the same objective lens. The reflected and re-collimated beam passes through the PBS, since it passed the quarter wave plate (QWP) twice and is horizontally polarized. The beam enters the telescope optics, the first polarizer, the calcite plate, the second polarizer, and collecting lens. The collecting lens focuses the beam on the pinhole aperture and the beam passing through the aperture is detected by the photon detector.

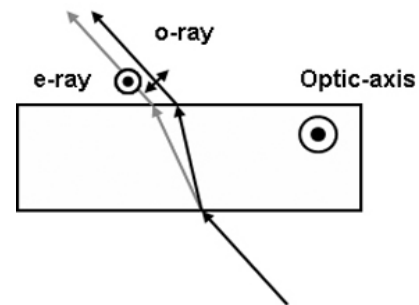
The calcite plate has different refractive indices along two perpendicular polarization directions. Thus, the propagation angle in the calcite plate differs as the polarization state of the entering beams differs, and this difference of the angles makes phase difference between two beams. This phase difference changes as the angle of incidence onto the calcite plate changes. The off-axial point in the specimen coherently scatters the focused beam, and this coherently scattered beam propagates with non-zero angle with respect to the optical axis. As the coherently scattering point changes in the specimen plane, the angle of propagation changes, and thus the phase difference induced by the calcite plate. This change of phase difference produces interference pattern along one direction in specimen coordinate. The telescope optic is used to magnify the incidence angle onto the calcite plate. Two polarizers are aligned crossed to each other and  $45^\circ$  with respect to the characteristic

polarization axis of the calcite plate to achieve the best visibility [8].

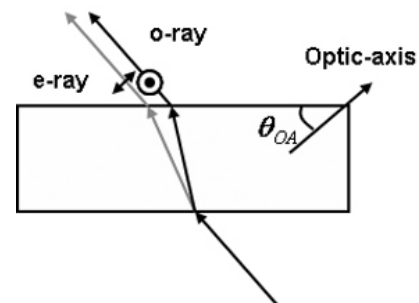
### III. ANALYSIS

The difference between the calcite plate in previous research and that in this paper is illustrated in Fig. 2. The main difference between these two calcite plates is direction of optic-axis. In Fig. 2 (a), the optic axis is perpendicular to the propagation direction and the boundary surface. Since the propagation vector of the e-ray is always perpendicular to the optic axis, the refractive index of the e-ray doesn't change. However, in Fig. 2 (b), the angle between the propagation vector of the e-ray and optic axis changes, as the incidence angle changes. This results in variation of refractive index of the e-ray according to the change of the incidence angle. The variation of the refractive index of the e-ray is an important factor of making different performance. For type B calcite plate, the optic axis angle  $\theta_{OA}$  is an important to determine the system performance. This optic axis angle is found to be  $45^\circ$  for type B calcite plate.

In CSIM, the most important factor of the performance is the sensitivity of the optical path difference (OPD) between the two perpendicularly polarized beams relative to the change of the incidence angle. The change of the OPD relative to the change of the incidence angle is plotted in Fig. 3. In this figure, the dotted and solid lines represent the OPD's of Type A and Type B calcite



(a) Calcite plate in previous research (Type A).



(b) Commercially available calcite plate (Type B).

FIG. 2. Difference between two calcite plates.

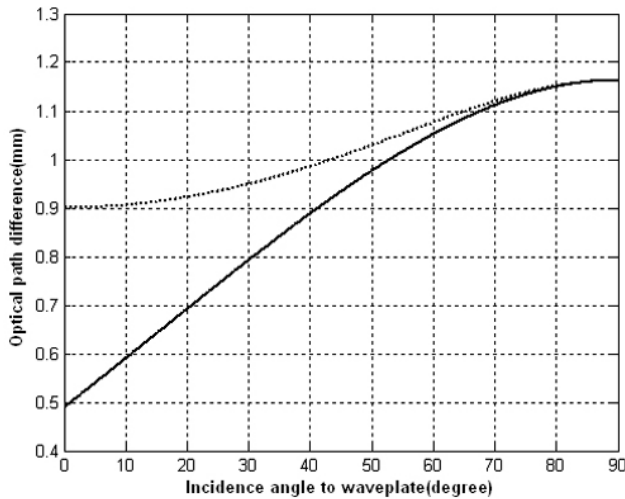


FIG. 3. OPD as a function of incidence angle (dotted line : Type A calcite plate, solid line : Type B calcite plate).

plates respectively. As can be shown from this figure, the slope of the curve for Type B calcite plate, which is the sensitivity of the OPD, is steeper than that for Type A calcite plate.

The sensitivity of the OPD is plotted in Fig. 4. As can be shown from this figure, the sensitivity for Type B calcite plate is larger than that for Type A calcite plate for the small value of the incidence angle. The maximum value of sensitivity for Type A calcite plate is lower than that for Type B calcite plate.

The increased sensitivity for Type B calcite plate is explained as follows. The exact expression of the OPD has been derived in previous publication, [7] but it can be simplified as follows:

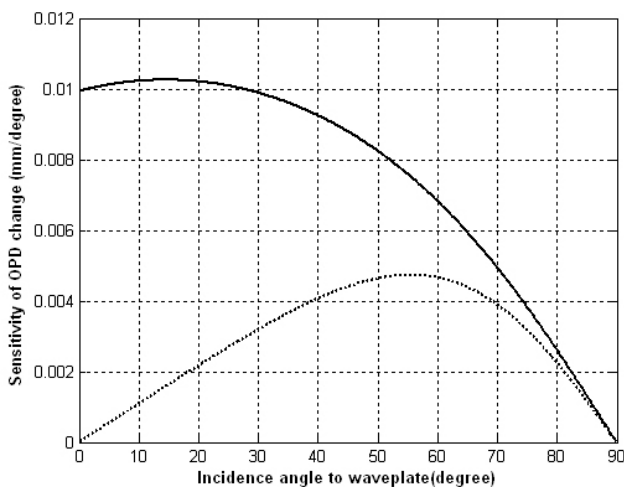


FIG. 4. Sensitivity of OPD as a function of incidence angle (dotted line : Type A calcite plate, solid line : Type B calcite plate).

$$\Delta S = n_o f_1(\theta) + f_2(\theta) - n_e(\theta) f_3(\theta), \quad (1)$$

where,  $n_o$  is the refractive index for the o-ray,  $\theta$  is incidence angle,  $f_1$ ,  $f_2$ , and  $f_3$  are positive valued geometrical functions of  $\theta$ , and  $n_e$  is the refractive index for the e-ray. Except for  $n_e$ , functions for Type A and Type B calcite plates have similar values and trends to each other. For Type A calcite plate,  $n_e$  is a constant value regardless of  $\theta$ , but for Type B calcite,  $n_e$  is a function of  $\theta$ . As can be shown from Fig. 5,  $n_e$  decreases as the incidence angle increases. Thus the OPD grows faster at small values of the incidence angle for Type B calcite plate than for Type A calcite plate.

The increased sensitivity shows lots of possible improvements when using Type B calcite plate. First, light efficiency can be improved. Since the large sensitivity can be achieved under normal incidence condition, reflection coefficients for both e- and o- rays are very low. Using Fresnel's law of reflection, we could achieve almost 90% light efficiency after two interfaces. Fig. 6 shows the visibility of the interference pattern when using Type B calcite plate. As can be shown from this figure, visibility of almost 1 can be easily achieved under normal incidence condition.

Second, the tight requirement for alignment can be loosened. In case of Type B calcite plate, the sensitivity is large over a range from  $0^\circ$  to  $30^\circ$ . When using Type A calcite plate as in previous research, the alignment is very important factor, since the sensitivity drops more quickly as the nominal angle departs from the optimal value around  $55.8^\circ$ .

#### IV. NUMERICAL EXPERIMENTS

The interference pattern induced by the change of incidence angle is shown in Fig. 7. For Type B calcite

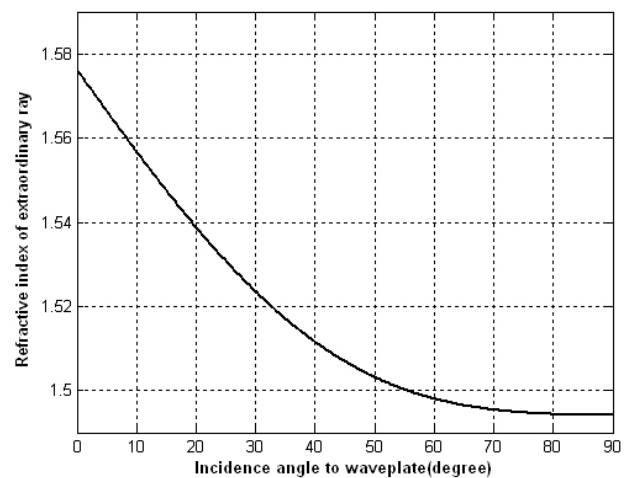


FIG. 5. Change of refractive index for e-ray as a function of incidence angle.

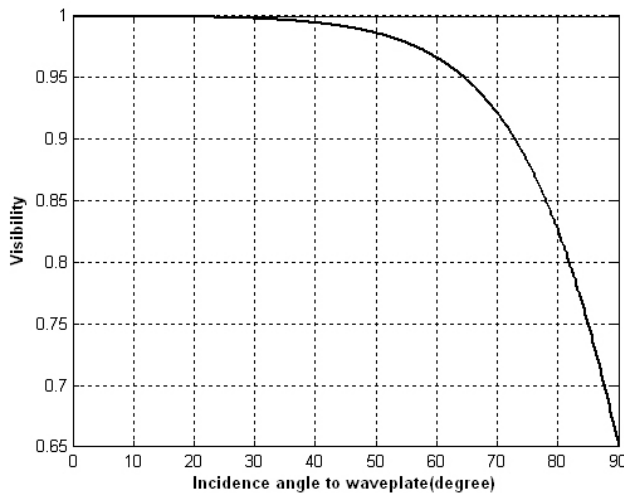


FIG. 6. Visibility of the interference pattern as a function of incidence angle.

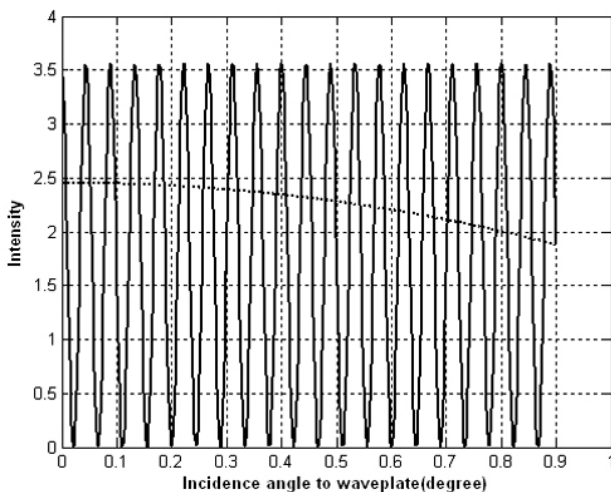


FIG. 7. Self-interference pattern (dotted line : Type A calcite plate, solid line : Type B calcite plate).

plate, the period of the interference pattern is very short, but for Type A calcite plate, one full pattern of the interference can hardly be seen. This shows that with Type B calcite plate central lobe of the PSF can be more sharpened than with Type A calcite plate.

## V. CONCLUSIONS

In this paper, we have proposed CSIM with commercially available calcite plate, which has its optic axis in the plane of incidence. We analyzed the characteristics of Type B calcite plate and compared the performances of two different type of calcite plates. With Type B calcite plate, very high sensitivity can be achieved under normal incidence condition, which improves the light efficiency.

However, in Type B calcite plate, the wavefront of the e-ray is not sphere, which causes lateral displacement of the e-ray at the exit surface of Type B calcite plate. This could invoke the unwanted interference pattern on the detector plane. To reject possible detector plane interference, a circular aperture, which only passes the overlapped area of two beams, can be used.

This research has been supported by the Korea Industrial Technology Foundation (KOTEF).

\*Corresponding author : godogo@kaist.ac.kr

## REFERENCES

- [1] J. B. Pawley, *Handbook of biological confocal microscopy* (Plenum Press, New York, 1995).
- [2] M. Vaez-iravani and D. I. Kavaldjiev, "Resolution beyond the diffraction limit using frequency-domain field confinement in scanning microscopy," *Ultramicroscopy* vol. 61, pp. 105-110, 1995.
- [3] C. J. R. Sheppard, "Binary optics and confocal imaging," *Opt. Lett.* vol. 24, no. 8, pp. 505-507, 1999.
- [4] M. A. A. Neil, R. Juskaitis, T. Wilson and Z. J. Laczik, "Optimized pupil-plane filters for confocal microscope point-spread function engineering," *Opt. Lett.* vol. 25, no. 4, pp. 245-247, 2000.
- [5] L. Liu, X. Deng, L. Yang, G. Wang, and Z. Xu, "Effect of an annular pupil filter on differential confocal microscopy," *Opt. Lett.* vol. 25, no. 23, pp. 1711-1713, 2000.
- [6] S. W. Hell, M. Schrader, and H. T. M. Van Der Voort, "Far-field fluorescence microscopy with three-dimensional resolution in the 100-nm range," *J. Microsc.-Oxford*, vol. 187, no. 1, pp. 1-7, 1997.
- [7] D. Kang and D. Gweon, "Enhancement of lateral resolution in confocal self-interference microscopy," *Opt. Lett.* vol. 28, no. 24, pp. 2470-2472, 2003.
- [8] M. Born and E. Wolf, *Principles of Optics* (Cambridge University Press, UK, 1999).